

The impact of cored density profiles on the observable quantities of dwarf spheroidal galaxies

David Harvey,¹★ Yves Revaz,¹ Andrew Robertson² and Loic Hausammann¹

¹Laboratoire d'Astrophysique, EPFL, Observatoire de Sauverny, CH-1290 Versoix, Switzerland

²Institute for Computational Cosmology, Durham University, South Road, Durham DH1 3LE, UK

Accepted 2018 August 29. Received 2018 August 13; in original form 2018 May 29

ABSTRACT

We modify the chemo-dynamical code GEAR to simulate the impact of self-interacting dark matter (SIDM) on the observable quantities of 19 low-mass dwarf galaxies with a variety star-forming properties. We employ a relatively high, velocity independent cross-section of $\sigma/m = 10 \text{ cm}^2 \text{ g}^{-1}$ and extract, in addition to integrated quantities, the total mass density profile, the luminosity profile, the line-of-sight velocities, the chemical abundance, and the star formation history. We find that despite the creation of large cores at the centre of the dark matter haloes, the impact of SIDM on the *observable* quantities of quenched galaxies is indiscernible, dominated mostly by the stochastic build up of the stellar matter. As such we conclude that it is impossible to make global statements on the density profile of dwarf galaxies from single or small samples. Although based mostly on quenched galaxies, this finding supports other recent work putting into question the reliability of inferred cored density profiles that are derived from observed line-of-sight velocities.

Key words: galaxies: dwarf – galaxies: evolution – Local Group – dark matter.

1 INTRODUCTION

For the last twenty years it has been argued two major observations have caused a ‘small-scale crisis’ in cosmology. The first is that the central regions of observed dwarf spheroidals have flat density profiles (a core), where CDM predicts centrally rising profiles (a cusp) (Dubinski & Carlberg 1991; Navarro, Frenk & White 1996, 1997) and the second is that there appears to be insufficient dark matter in the most massive subhaloes (Klypin et al. 1999; Moore et al. 1999; Boylan-Kolchin, Bullock & Kaplinghat 2011). However, more recently it has been noted that these structures are very sensitive to baryonic physics and environmental processes, altering the total density profile changing a cusp to a core (Pontzen & Governato 2014) and tidal stripping and ram pressure can disrupt haloes bringing the expected number of observed small haloes down considerably (Sawala et al. 2016; Wetzel et al. 2016). On the other-hand, even taking into account the unknown effects of baryons, some studies of dwarf galaxies have argued that discrepancies may possibly persist (Schneider et al. 2017) and these inconsistencies can be attributed to an incomplete description of dark matter (Spergel & Steinhardt 2000; Lovell et al. 2012; Rocha et al. 2013; Zavala, Vogelsberger & Walker 2013). As a result it remains unclear whether there exists such a ‘crisis’ or whether observations have been misinterpreted (Verbeke et al. 2017).

In this letter, we modify a suite of dwarf spheroidal galaxy simulations to simulate the impact of self-interacting dark matter (SIDM) on their observable quantities and quantify exactly how well these objects can be used to understand the nature of dark matter.

SIDM in recent times has been of increased interest both theoretically and observationally. Theoretically it can thermalize haloes, creating cores, and also potentially reduce the amount of substructure (Peter et al. 2013; Rocha et al. 2013; Buckley et al. 2014; Vogelsberger et al. 2016), and hence ease the apparent tensions. Observationally, high-resolution space-based imaging of large samples of galaxy clusters has meant that now we can probe this fundamental property down to $\sigma/m \sim 1 \text{ cm}^2 \text{ g}^{-1}$ (e.g. Markevitch et al. 2004; Harvey et al. 2015; Massey et al. 2017; Robertson, Massey & Eke 2017), however, tight constraints from low-mass haloes remain sparse.

Given the nature of Dwarf Spheroidals and the peak in interest in SIDM, the number of studies looking at simulations of SIDM at the dwarf galaxy scale has naturally grown. Vogelsberger et al. (2014) originally studied two dwarf galaxies with both a constant and velocity dependent cross-section. Studying relatively large dwarf galaxies ($M_{\text{halo}} \sim 10^{10} M_{\odot}$, $M_{\star} \sim 10^8 M_{\odot}$) they found that self-interactions had minimal impact on the global properties of the dwarf galaxies. However they did find that the metallicity in the centre rose by 15 per cent and the stellar distribution traced that of the cored dark matter. Following this, the Feedback In Realistic Environments (FIRE) simulations simulated four dwarf galaxies including SIDM (Robles et al. 2017). This study looked at smaller mass dwarf galaxy-

* E-mail: david.harvey@epfl.ch

ies finding that even the smallest haloes ($< 3 \times 10^6 M_\odot$) formed cores, which were relatively unaffected by baryonic physics. Although seminal to SIDM work, these studies lacked two important characteristics. The first is the small sample sizes meant they could not probe the diversity of profiles within a range of dwarf galaxies from a variety of formation histories. Secondly these studies did not calculate the impact on the direct observables, including the line-of-sight (LOS) velocities of stars within the haloes and verify that the metallicity abundances were consistent with observations.

In this letter, we therefore look to extend this work, simulating a larger suite of dwarf galaxies using the chemo-dynamical code GEAR (Revaz & Jablonka 2012; Revaz et al. 2016). Recently, Revaz & Jablonka (2018) demonstrated that cosmological simulations with GEAR reproduced the details of a wide range of observable quantities of dwarf galaxies, including LOS velocity dispersion profiles, half-light radii, star formation histories, metallicity distributions, [Mg/Fe] abundance ratios, metallicity gradients, and kinetically distinct stellar populations. It is therefore now possible to fully test the impact of more exotic models of dark matter. In particular, we will study for the first time how SIDM influences these observables.

2 SIMULATIONS

GEAR (Revaz & Jablonka 2012; Revaz et al. 2016) is a fully parallel chemo-dynamical Tree/SPH code based on Gadget-2 (Springel 2005). It includes gas cooling, hydrogen self-shielding, star formation, chemical evolution, and Type Ia and II supernova yields and thermal blastwave-like feedback. GEAR includes recent and essential SPH improvements like the pressure-entropy formulation (Hopkins 2013) and operates with individual and adaptive time-steps as described in Durier & Dalla Vecchia (2012).

For the purpose of this study, we extend GEAR to include SIDM. Following Robertson et al. (2017), we implement isotropic and velocity-independent scattering of dark matter particles, using a relatively large cross-section of $\sigma/m = 10 \text{ cm}^2 \text{ g}^{-1}$ to maximize any effect.

To check the impact of SIDM on dwarf galaxies' properties, we selected 19 haloes from Revaz & Jablonka (2018) and re-simulate them with our SIDM prescription. The selection is performed to cover the three different types of star formation histories defined in Revaz & Jablonka (2018), namely: sustained, extended and quenched. Sustained star formation histories produce bright dwarfs ($L_V > 10^8 L_\odot$) which due to our high-mass resolution ($m_\star = 1024 M_\odot \text{ h}^{-1}$) require substantial CPU resources.¹ Conversely, quenched galaxies are faint ($L_V < 10^6 L_\odot$) and much quicker to simulate. We therefore simulate sixteen quenched galaxies, one sustained one (h019) and two extended ones (h050 and h070), in an identical manner (except the inclusion of dark matter scattering) to their counterparts in Revaz & Jablonka (2018).

3 RESULTS

Table 1 gives an overview of the results. For each column we show the CDM value followed by the SIDM value for the same halo. Throughout we split our sample into three star-forming classes: sustained, extended, and quenched as shown in the final column of this table.

¹For those bright galaxies that continuously form stars, owing to the large sound speed of the feedback-heated dense gas, the time-step may drop below 1000 yr.

In Fig. 1, we show the radial dependence of four different properties for the three samples of dwarf galaxies at $z = 0$. The left-hand column gives the sustained star-forming galaxy, the middle column gives the two extended star-forming galaxies, and the final column gives the distribution of the 16 quenched galaxies, giving the region in which 68 per cent of these galaxies lie. We also delineate the 2.8 times Plummer-equivalent gravitational softening length for the dark matter particles in the simulation, value beyond which the gravitational forces are Newtonian.

The top row shows the total matter density profile. In all but the sustained star-forming galaxy we find that SIDM leads to cored density profiles, while CDM has larger central densities, also shown in the dark matter only profiles. Interestingly the core is unobservable in the total matter profile of h019 suggesting that the additional stellar component dominates in these galaxies and is also cored.

Investigating h019 further, we find that the mass within 300pc doubles in the final 2 Gyr. This effect could be due to core collapse from a very high cross-section (Elbert et al. 2018). However, h019 is complicated, experiencing a major merger and as such particularly difficult to interpret.

Despite the dramatic difference between CDM and SIDM, we find that the projected luminosity profiles do not differ noticeably as shown in the third row. Interestingly, we find that SIDM in h050 has the opposite effect to what is expected. The SIDM increases the luminosity of this galaxy despite having a cored dark matter density, demonstrating the stochasticity during the formation of stars and how their dynamics are only weakly coupled to the dark matter. Finally, the quenched galaxies exhibit overlapping distributions, meaning that it would be impossible to differentiate between SIDM and CDM in these small, low-mass haloes.

The final row shows the LOS velocity profiles. We find that the sustained star-forming galaxy is slightly lower for the SIDM than the CDM. Although the total mass is the same, this difference might be the result of late time formation of stars within a cored halo resulting in this lower velocity. The middle column presents a somewhat unclear conclusion. Although h070 reacts to the drop in total density by exhibiting a lower velocity profile, halo h050 clearly has an indistinguishable velocity profile, despite also having reduced total and dark matter densities. We postulate that although these galaxies can have very different density profiles, stochastic build up of the stellar matter at early times in the central regions can cause CDM to mimic the observables of cored profiles in SIDM. The final column shows overlapping distributions, suggesting that it is common for dwarfs to have similar velocity profiles despite harbouring a factor of ~ 5 difference in total density.

Following these tests we carry out two further studies. The top row of Fig. 2 shows the impact of SIDM on the metallicity distribution of stars in the galaxies. To derive these distributions, we sum each metallicity density distributions at $z = 0$ and took the mean. The bottom row gives integrated star formation rate normalized to the total halo mass as a function of cosmic time. We again give the region in which 68 per cent of the galaxies lie. We find in star-forming cases there is no clear differentiation between the two models and that the creation of a core in the total mass profile does not alter the chemical evolution of the dwarf galaxies *on the whole*. The two haloes that experience extended star formation have a slightly higher mean metallicity with SIDM, however the difference is only small, and so potentially unreliable with only two haloes.

Table 1. A direct comparison between 19 simulated dwarf galaxies with CDM and the corresponding halo with SIDM (i.e. CDM / SIDM). From left to right the columns give the halo ID, the total V-band luminosity within R_{200} , the total stellar mass within R_{200} , the total mass within R_{200} , the total gas mass within R_{200} , R_{200} (the radius at which the mean enclosed density is 200 times the critical density), the mean LOS velocity, and the metallicity. The final column gives the classification of star formation whether it is sustained, extended or quenched.

Model ID	L_v [$10^6 L_\odot$]	M_\star [$10^6 M_\odot$]	M_{200} [$10^9 M_\odot$]	M_{gas} [$10^6 M_\odot$]	R_{200} [kpc]	σ_{LOS} [km/s]	[Fe/H] [dex]	SF Class
h019	291/283	434/404	9.5/9.4	280/315	50.7/50.5	30.5/28.8	-0.6/-0.5	Sustained
h050	4.2/7.1	9.6/13.7	2.6/2.7	15.1/20.2	33.0/33.2	10.4/10.8	-1.3/-1.3	Extended
h070	2.0/2.0	5.8/5.9	1.8/1.8	0.0/1.5	29.2/29.3	10.8/10.3	-1.5/-1.4	Extended
h132	0.7/0.7	2.1/2.1	0.9/0.9	0.5/0.6	23.1/23.0	9.3/9.0	-2.1/-2.0	Quenched
h074	0.5/0.5	1.3/1.2	0.7/0.7	0.4/0.5	21.2/21.1	9.1/8.5	-2.1/-2.2	Quenched
h159	0.4/0.4	1.1/1.0	0.7/0.7	0.0/0.0	21.0/21.0	8.9/9.5	-2.3/-2.3	Quenched
h064	0.4/0.4	1.1/1.1	1.9/1.8	5.2/5.0	29.5/29.3	9.7/8.7	-1.9/-1.9	Quenched
h059	0.3/0.2	0.7/0.6	2.1/2.1	4.2/4.3	30.5/30.5	9.3/8.9	-2.4/-2.2	Quenched
h141	0.2/0.2	0.6/0.6	0.8/0.8	0.5/0.7	21.8/21.9	8.3/8.1	-2.2/-2.4	Quenched
h061	0.2/0.2	0.5/0.6	1.9/2.0	3.4/3.6	29.8/30.0	9.1/9.6	-2.1/-2.1	Quenched
h111	0.2/0.2	0.5/0.4	1.1/1.1	0.1/0.3	24.6/24.6	10.4/10.5	-2.4/-2.4	Quenched
h177	0.2/0.2	0.5/0.5	0.5/0.5	0.0/0.0	19.4/19.4	7.7/7.9	-2.6/-2.3	Quenched
h091	0.2/0.2	0.4/0.4	1.4/1.3	0.8/0.7	26.5/26.3	10.1/8.2	-1.9/-2.5	Quenched
h106	0.2/0.1	0.4/0.3	1.1/1.1	0.1/0.1	24.6/24.5	9.9/8.3	-2.8/-2.3	Quenched
h122	0.1/0.1	0.4/0.3	1.0/1.0	0.0/0.0	23.7/23.7	9.1/9.2	-2.4/-2.5	Quenched
h104	0.1/0.1	0.3/0.4	0.9/0.9	0.3/0.1	23.3/23.0	9.0/8.5	-2.3/-2.4	Quenched
h123	0.1/0.2	0.3/0.4	0.9/0.9	0.1/0.0	23.2/23.1	7.6/7.6	-2.2/-2.3	Quenched
h180	0.1/0.1	0.3/0.3	0.3/0.3	0.0/0.0	15.9/15.7	6.9/6.9	-2.4/-2.3	Quenched
h168	0.1/0.1	0.3/0.3	0.6/0.6	0.0/0.1	19.7/19.6	8.3/9.0	-2.6/-2.5	Quenched

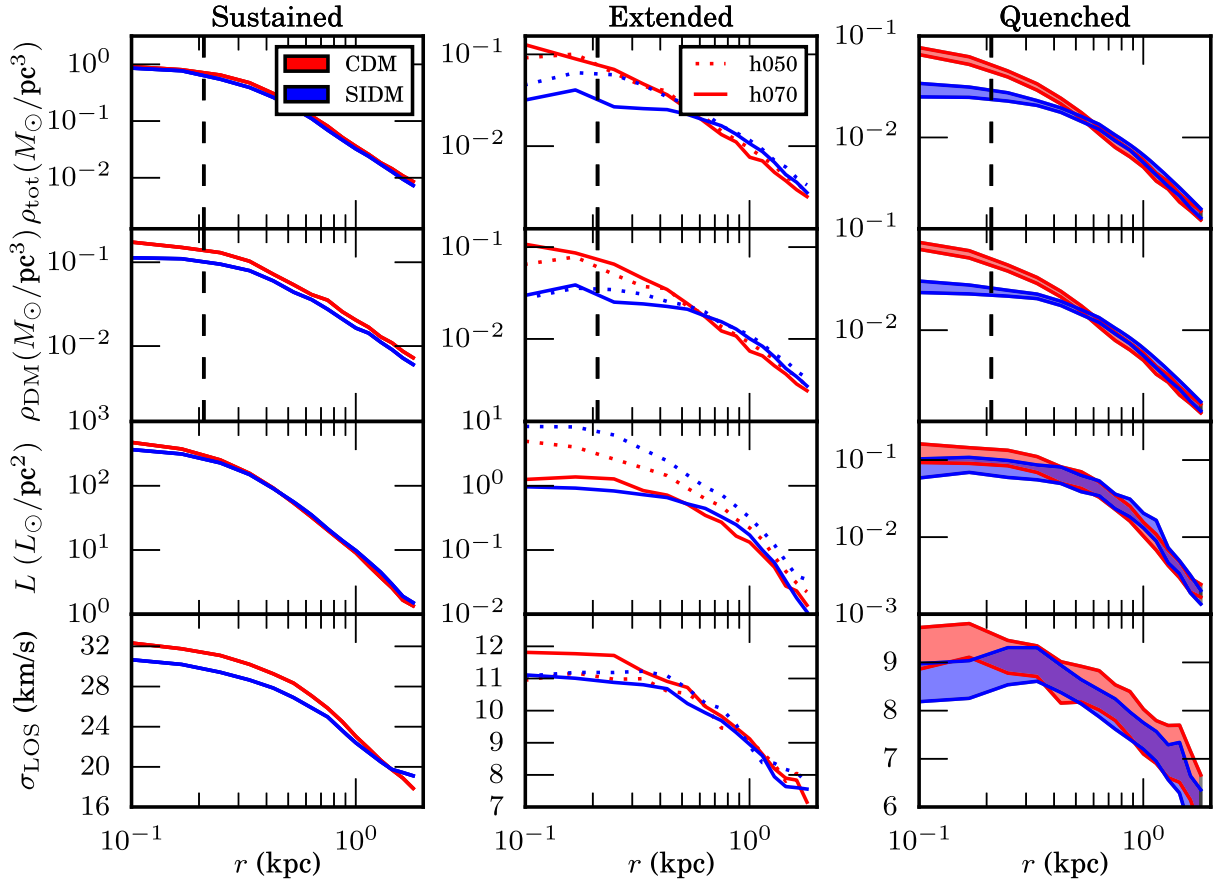


Figure 1. Four radial-dependent properties of the three samples of dwarf galaxies at $z = 0$ with the CDM model in red and the SIDM in blue. The left-hand column gives the sustained star forming and the middle column gives the two extended star forming. The final column gives the shaded region within which 68 per cent of the 16 quenched galaxies lie. The vertical dashed line corresponds to 2.8 times the softening length of the dark matter particles. From top to bottom the rows give (1) the total mass density profile, (2) the dark matter density profile, (3) the luminosity surface density, and (4) the LOS velocity profile of the stars.

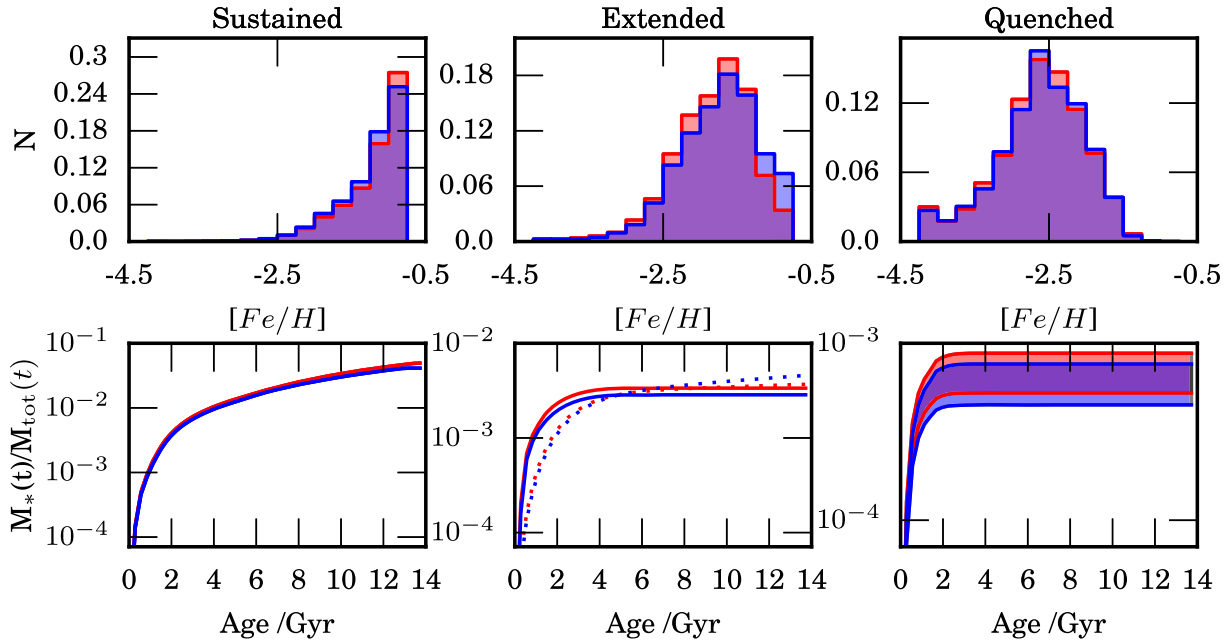


Figure 2. Same columns as Fig. 1. The first row gives the metallicity density function and the second gives the integrated star formation history normalized to the total mass of the halo.

3.1 Time evolution of the line-of-sight velocities

It is striking from Fig. 1 that although the total mass within the central region changes significantly with SIDM, we find little change in the stellar LOS velocities. We postulate this is because the observable quantities of the stars are defined by the potential in which they are formed, when the halo harbours a cusp. To examine this further we study the time evolution of the mass within 300 pc of three dwarf galaxies and the stellar LOS velocity at the same radii. Fig. 3 shows the results. Each panel presents the results from a single dwarf galaxy with the CDM (SIDM) results in red (blue). The shaded region shows the evolution of the LOS velocities over cosmic time with the 1σ error and the solid lines shows the total mass within a 3D radius of 300 pc. We clearly see the core developing, with the SIDM mass departing from the CDM mass over time. However, the LOS velocity remains unchanged from its initial values, only mildly evolving with time. We conclude that the impact on the LOS velocity due to a redistribution of the central dark matter is imperceptible. This conclusion is confirmed by a Jeans prediction of the velocity dispersion of our simulated dwarfs.

4 DISCUSSION AND CONCLUSIONS

We simulate a suite of 19 dwarf spheroidal galaxies using a modified version of the chemo-dynamical code GEAR to include self-interacting dark matter. We simulate a velocity independent cross-section of $\sigma/m = 10 \text{ cm}^2 \text{ g}^{-1}$ with a three regimes of star formation and extract four observable quantities: the luminosity and the LOS velocity profile, the metallicity abundance, and the integrated star formation history. In general, we find the change in dark matter model changes the individual evolution of each galaxy, with each dwarf spheroidal forming a dark matter core in the central region. However, despite this the distribution of the 16 quenched galaxies does not and that there is no discernible difference in observable quantities. We postulate that this due to the stochastic nature of early star formation within the galaxy and are henceforth defined by its

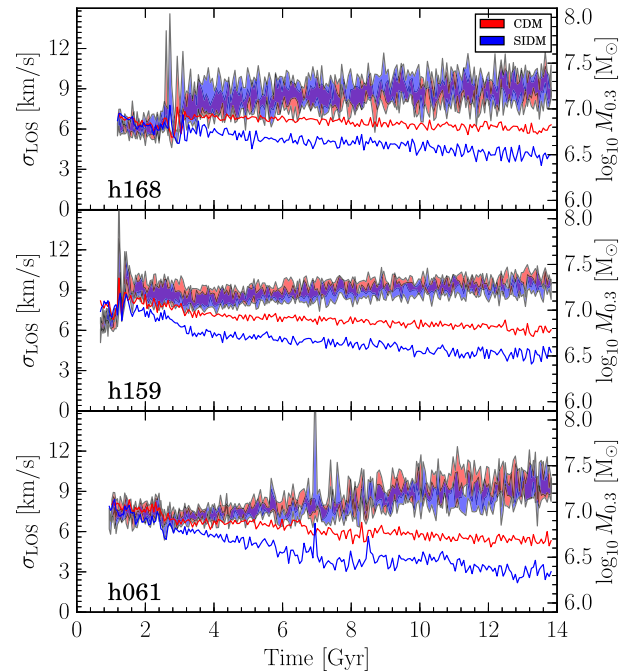


Figure 3. The time evolution of the LOS velocity of stars at 500 pc from the centre of the halo and its associated 1σ error for three dwarf galaxies. The solid line is the time evolution of the integrated mass inside the same radius. The red are the dwarf galaxies with CDM and the blue is the SIDM.

initial potential and are insensitive to the redistribution of matter caused by SIDM. Although the limited number of extend and sustained star-forming dwarf galaxies prevent us from extrapolating this conclusion to these galaxy types, we do find large variances in the formation history of these galaxies and therefore raise caution to studies making global statements about dwarf galaxies based on observations of single or small samples. Although based on our

sample of quenched dwarf spheroidals, this finding is consistent with other studies of dwarf galaxies that puts in to questions the reliability of the interpretations from observations that dwarf galaxies harbour cored density profiles (Strigari, Frenk & White 2017) and that a small-scale crisis exists in cosmology.

ACKNOWLEDGEMENTS

This research is supported by the Swiss National Science Foundation (SNSF). DH also acknowledges support by the Merac foundation. AR is supported by a European Research Council Starting Grant (ERC-StG-716532-PUNCA).

REFERENCES

- Boylan-Kolchin M., Bullock J. S., Kaplinghat M., 2011, *MNRAS*, 415, L40
- Buckley M. R., Zavala J., Cyr-Racine F.-Y., Sigurdson K., Vogelsberger M., 2014, *Phys. Rev. D*, 90, 043524
- Dubinski J., Carlberg R. G., 1991, *ApJ*, 378, 496
- Durier F., Dalla Vecchia C., 2012, *MNRAS*, 419, 465
- Elbert O. D., Bullock J. S., Kaplinghat M., Garrison-Kimmel S., Graus A. S., Rocha M., 2018, *ApJ*, 853, 109
- Harvey D., Massey R., Kitching T., Taylor A., Tittley E., 2015, *Science*, 347, 1462
- Hopkins P. F., 2013, *MNRAS*, 428, 2840
- Klypin A., Kravtsov A. V., Valenzuela O., Prada F., 1999, *ApJ*, 522, 82
- Lovell M. R., Eke V., Frenk C. S. et al., 2012, *MNRAS*, 420, 2318
- Markevitch M., Gonzalez A. H., Clowe D., Vikhlinin A., Forman W., Jones C., Murray S., Tucker W., 2004, *ApJ*, 606, 819
- Massey R. et al., 2018, *MNRAS*, 477, 669
- Moore B., Ghigna S., Governato F., Lake G., Quinn T., Stadel J., Tozzi P., 1999, *ApJ*, 524, L19
- Navarro J. F., Frenk C. S., White S. D. M., 1996, *ApJ*, 462, 563
- Navarro J. F., Frenk C. S., White S. D. M., 1997, *ApJ*, 490, 493
- Peter A. H. G., Rocha M., Bullock J. S., Kaplinghat M., 2013, *MNRAS*, 430, 105
- Pontzen A., Governato F., 2014, *Nature*, 506, 171
- Revaz Y., Jablonka P., 2012, *A&A*, 538, A82
- Revaz Y., Jablonka P., 2018, *A&A*, 616, A96
- Revaz Y., Arnaudon A., Nichols M., Bonvin V., Jablonka P., 2016, *A&A*, 588, A21
- Robertson A., Massey R., Eke V., 2017, *MNRAS*, 465, 569
- Robles V. H., et al., 2017, *MNRAS*, 472, 2945
- Rocha M., Peter A. H. G., Bullock J. S., Kaplinghat M., Garrison-Kimmel S., Onorbe J., Moustakas L. A., 2013, *MNRAS*, 430, 81
- Sawala T. et al., 2016, *MNRAS*, 457, 1931
- Schneider A., Trujillo-Gomez S., Papastergis E., Reed D. S., Lake G., 2017, *MNRAS*, 470, 1542
- Spergel D. N., Steinhardt P. J., 2000, *Phys. Rev. Lett.*, 84, 3760
- Springel V., 2005, *MNRAS*, 364, 1105
- Strigari L. E., Frenk C. S., White S. D. M., 2017, *ApJ*, 838, 123
- Verbeke R., Papastergis E., Ponomareva A. A., Rath S., De Rijcke S., 2017, *A&A*, 607, A13
- Vogelsberger M., Zavala J., Simpson C., Jenkins A., 2014, *MNRAS*, 444, 3684
- Vogelsberger M., Zavala J., Cyr-Racine F. Y., Pfrommer C., Bringmann T., Sigurdson K., 2016, *MNRAS*, 460, 1399
- Wetzel A. R., Hopkins P. F., Kim J. -h., Faucher-Giguère C. A., Kereš D., Quataert E., 2016, *ApJ*, 827, L23
- Zavala J., Vogelsberger M., Walker M. G., 2013, *MNRAS*, 431, L20

This paper has been typeset from a \LaTeX file prepared by the author.